OPEN

Cell Death and Differentiation (2016) 23, 1529–1541
Official journal of the Cell Death Differentiation Association

www.nature.com/cdd

β-Arrestin-2 modulates radiation-induced intestinal crypt progenitor/stem cell injury

Z Liu[1,2,3], H Tian[1,2], J Jiang[1], Y Yang[1], S Tan[1], X Lin[1], H Liu[1] and B Wu*[,1]

Intestinal crypt progenitor/stem (ICPS) cell apoptosis and vascular endothelial cell apoptosis are responsible for the initiation and development of ionizing radiation (IR)-evoked gastrointestinal syndrome. The signaling mechanisms underlying IR-induced ICPS cell apoptosis remain largely unclear. Our findings provide evidence that β-arrestin-2 (βarr2)-mediated ICPS cell apoptosis is crucial for IR-stimulated intestinal injury. *βArr2*-deficient mice exhibited decreased ICPS cell and intestinal Lgr5$^+$ (leucine-rich repeat-containing G-protein-coupled receptor 5-positive) stem cell apoptosis, promoted crypt proliferation and reproduction, and protracted survival following lethal doses of radiation. Radioprotection in the ICPS cells isolated from *βarr2*-deficient mice depended on prolonged nuclear factor-κB (NF-κB) activation via direct interaction of βarr2 with IκBα and subsequent inhibition of p53-upregulated modulator of apoptosis (PUMA)-mediated mitochondrial dysfunction. Unexpectedly, *βarr2* deficiency had little effect on IR-induced intestinal vascular endothelial cell apoptosis in mice. Consistently, βarr2 knockdown also provided significant radioresistance by manipulating NF-κB/PUMA signaling in Lgr5$^+$ cells *in vitro*. Collectively, these observations show that targeting the βarr2/NF-κB/PUMA novel pathway is a potential radiomitigator for limiting the damaging effect of radiotherapy on the gastrointestinal system. Significance statement: acute injury to the intestinal mucosa is a major dose-limiting complication of abdominal radiotherapy. The issue of whether the critical factor for the initiation of radiation-induced intestinal injury is intestinal stem cell apoptosis or endothelial cell apoptosis remains unresolved. βArrs have recently been found to be multifunctional adaptor of apoptosis. Here, we found that β-arrestin-2 (βarr2) deficiency was associated with decreased radiation-induced ICPS cell apoptosis, which prolonged survival in abdominally irradiated mice. Moreover, *βarr2* deficiency-mediated intestinal progenitor/stem cell radioprotection relied on protracted NF-κB activation and subsequent suppression of PUMA induction. Our results suggest that ICPS cell apoptosis is the factor involved in the initiation and development of radiation-induced gastrointestinal syndrome. βArr2 is a potential target for lessening radiation-induced ICPS cell apoptosis.

Cell Death and Differentiation (2016) **23,** 1529–1541; doi:10.1038/cdd.2016.38; published online 29 April 2016

Gastrointestinal (GI) syndrome is the primary radiotherapy-associated complication in clinical use and efficacy of ionizing radiation (IR) for treating abdominal and pelvic cancers.[1] The underlying molecular mechanism of IR-induced intestinal injury is still not well understood. Some researchers suppose that intestinal progenitor/stem cells, almost always located in crypts, subjected directly to IR insult are a crucial factor in the process.[2] However, their precise location and properties have been disputed in the absence of a definitive molecular marker. Various studies indicated that cells at position 4 in the intestinal crypt above Paneth cells are putative stem cells.[3,4] Recently, evidence obtained using genetic modification technology has convincingly shown that intestinal stem cells are columnar cells at the crypt base (CBCs) intermingling with Paneth cells.[5] Many have postulated that IR-induced apoptosis of putative intestinal stem cells, which reside at the +4 position from the crypt bottom or at the crypt base bottom, is the primary factor initiating GI syndrome, whereas others believe that the cells initially targeted by IR are vascular endothelial cells in the crypt–villus axis, and it then switches to intestinal stem cells.[2,6–9] Acid sphingomyelinase (ASMase)-mediated ceramide production in endothelial cells inside the villus was suggested to account for the initiation of GI syndrome. Deficiency in ASMase, treatment with basic fibroblast growth factor, which blocks ASMase in the endothelial cells, and systemic administration of anti-ceramide antibody ameliorated IR-induced endothelial apoptosis and thereby protected the intestine from IR-induced damage.[7–9] However, it is still unclear whether intestinal progenitor/stem cell apoptosis or endothelial cell apoptosis is the main factor involved in the initiation and development of IR-induced GI syndrome. Given that intestinal cell apoptosis has major implications in GI syndrome, radiation oncologists and medical researchers have been seeking radioprotective

[1]Department of Gastroenterology, The Third Affiliated Hospital of Sun Yat-sen University, Guangzhou, China
*Corresponding author: B Wu, Department of Gastroenterology, The Third Affiliated Hospital of Sun Yat-sen University, 600 Tianhe Road, Guangzhou 510630, China. Tel: +86 20 85252801; Fax: +86 20 85253336; E-mail: wubin6@mail.sysu.edu.cn
[2]These authors contributed equally to this work.
[3]Current address: Division of Emergence Medicine, Department of General Internal Medicine, The First Affiliated Hospital of Sun Yat-sen University, Guangzhou, China.

Abbreviations: ICPS, intestinal crypt progenitor/stem; βarrs, β-arrestins; NF-κB, nuclear factor-κB; PUMA, P53-upregulated modulator of apoptosis; GI, gastrointestinal; IR, ionizing radiation; CBC, columnar cells at the crypt base; ASMase, acid sphingomyelinase acid; LPS, lipopolysaccharide; TNFα, tumor necrosis factor-α; IκB, inhibitor of κB kinase; IKK, IκB kinase; Lgr5, leucine-rich repeat-containing G-protein-coupled receptor 5; EMSA, electrophoretic mobility shift assay; TUNEL, TdT-mediated dUTP nick-end labeling

Received 23.8.15; revised 14.3.16; accepted 21.3.16; Edited by R De Maria; published online 29.4.2016

agents for the intestine that would help to limit intestinal cell death and facilitate intestinal crypt reproduction. Several protective substances that minimize IR-induced intestinal apoptosis have been known for decades. Tumor necrosis factor-α (TNFα)[10] and bacterial lipopolysaccharide (LPS),[11] which are canonical activators of the nuclear factor-κB (NF-κB) pathway, have been shown to decrease intestinal epithelial radiosensitivity.

IR has been found to transiently activate NF-κB signaling cascades in the intestines.[12–16] NF-κBs, which are a family of transcription factors, have an important function in regulating cell antiapoptosis, cell proliferation and immune response.[17] Signaling cascades induced by LPS, interleukin-1, TNFα or DNA double-strand breaks activate the IκB kinase (IKK) complex, which phosphorylates inhibitor of κB (IκB) proteins leading to their degradation.[10,14] The series of signal transductions transfer the accumulated dissociative NF-κB from the cytoplasm into the nucleus, where it binds to the promoter regions of specific target genes that encode anti- and proapoptotic proteins.[17] It has been shown that LPS and toll-like 5 receptor agonist CBLB502, which both act as NF-κB-inducing agents, defend against IR-induced intestinal apoptosis in mice, but their intestinal radioprotection could be counteracted by the selective intestinal depletion of IKKβ.[14,18] Furthermore, mice genetically modified by the deletion of vital components of the NF-κB pathway containing p50 or IKKβ are hypersensitive to IR-induced intestinal apoptosis.[14,15] These findings imply that NF-κB activation decreases intestinal epithelial apoptosis and reduces intestinal radiosensitivity. The major mechanism by which NF-κB activation suppresses intestinal apoptosis following IR remains to be determined.

β-Arrestins (βarrs), including β-arrestin-1 (βarr1) and β-arrestin-2 (βarr2), are ubiquitous multifunctional adaptor proteins that were initially identified merely as negative regulators of the G-protein-coupled receptor pathway,[19] as their functions in signal pathways are somewhat diverse. However, over the past decade, numerous researches studies have confirmed that βarrs have indispensable roles as scaffolds and adaptors in apoptosis-associated signal transduction.[20–25] Accumulating evidence also suggests that βarrs function in the antiapoptotic pathway by influencing the activity of kinases.[20–22] In contrast, *in vitro*, βarrs have been shown to promote apoptosis under certain conditions by interacting with the p53, Mdm-2 or JNK pathway.[23–25] However, there are no reports on the exact mechanism and effect of βarrs on IR-induced intestinal apoptosis.

In this study, we found a critical role for βarr2, not βarr1, in regulating IR-induced apoptosis in the intestinal stem cell compartment and the pathogenesis of GI syndrome. By using genetic mice, we found that *βarr2* deficiency reduced intestinal crypt progenitor/stem (ICPS) cell apoptosis in response to IR and resulted in enhanced crypt regeneration and prolonged survival of mice subjected to lethal doses of IR. Furthermore, prolonged NF-κB activation following lethal IR in *βarr2* knockout (KO) mice alleviated GI syndrome by suppressing PUMA, whereas the NF-κB inhibitor Bay117082 was shown to aggravate GI syndrome by promoting PUMA. Our data robustly suggest that targeting the βarr2-mediated NF-κB pathway may be therapeutically useful to manipulate the response of the intestines to radiation in cancer patients.

Results

ICPS cell *β*arr expression and apoptosis-associated proteins in IR-treated mice. We found that *βarr2* mRNA was induced by ~4-fold at 24 h in ICPS cells after IR at 8, 15 and 18 Gy (Figure 1a), but βarr2 protein expression in ICPS cells was not distinctly changed at 4 and 24 h after three doses of IR (Figures 1b and c). Moreover, the expression of βarr1 in ICPS cells at neither the mRNA nor the protein level was affected by IR (Figures 1a and b). Furthermore, pro- and antiapoptotic proteins in ICPS cells were detected at 24 h after IR. The levels of p53, PUMA, Bax and Bcl-2 were elevated, whereas Bak and Bcl-X_L were not influenced following IR (Figures 1d and e). Importantly, the antiapoptotic protein NF-κB p65 in ICPS cells was increasingly translocated into the nucleus and actively bound at DNA sites at 4 h after IR (Figure 1f). However, the elevated translocation of NF-κB p65 and NF-κB DNA-binding activity in ICPS cells completely disappeared by 6 h after IR (Figure 1f). These results indicate that IR significantly induced βarr2, but not βarr1 mRNA, increased the expression of apoptosis-associated proteins and transiently activated the NF-κB pathway in ICPS cells of mice.

***βArr2* deficiency impaired IR-induced ICPS cell apoptosis.** To investigate the influence of βarrs on IR-induced GI syndrome, we treated βarrs WT and KO mice with IR. We found that IR at 15 Gy caused severe body weight loss and shortened the survival of βarrs WT mice, whereas the outcome was significantly improved in βarr2 KO mice, but not in βarr1 KO mice (Figures 1a and b and Supplementary Figures 1i and j). Next, we examined intestinal crypt apoptosis, which is closely associated with IR-induced GI syndrome. We observed that IR (8, 15 and 18 Gy) markedly induced ICPS cell apoptosis in WT mice, which was reduced by 57% at 24 h in *βarr2* KO mice, but not in *βarr1* KO mice (Figures 2c and e and Supplementary Figures 1a, b, g and h). In particular, apoptosis at cell positions 3–6 in the crypt was decreased by more than 40% and 50% in *βarr2* KO mice at 4 and 24 h after IR at 18 Gy, respectively (Figure 2h and Supplementary Figure 1f). The caspase-3 activity in ICPS cells was strikingly reduced in *βarr2* KO mice, compared with that in WT counterparts (Figure 2d and Supplementary Figures 1c and d). Remarkably, in WT counterparts, the intestinal stem cells at positions 3–6 from the crypt bottom were hypersensitive to radiation-induced apoptosis, and more than 90% of crypts contained apoptotic cells at positions 4–11 following IR at 18 Gy (Figures 2g and h). In contrast, the CBCs at positions 1–3 were relatively radioresistant, with 12%, 40%, 45% of crypts containing them after IR at 8, 15 and 18 Gy in WT mice, respectively (Figures 2g and h and Supplementary Figure 1e). *βArr2* KO also suppressed apoptosis in CBCs by nearly 50% at 4 h after IR at 15 and 18 Gy (Supplementary Figure 1e). These observations demonstrate that βarr2, but not βarr1, is an important mediator of IR-induced ICPS cell apoptosis.

Targeted deletion of βarr2 attenuated intestinal Lgr5$^+$ stem cell apoptosis in response to IR. To confirm the effect of βarr2 on radiation-induced apoptosis in intestinal

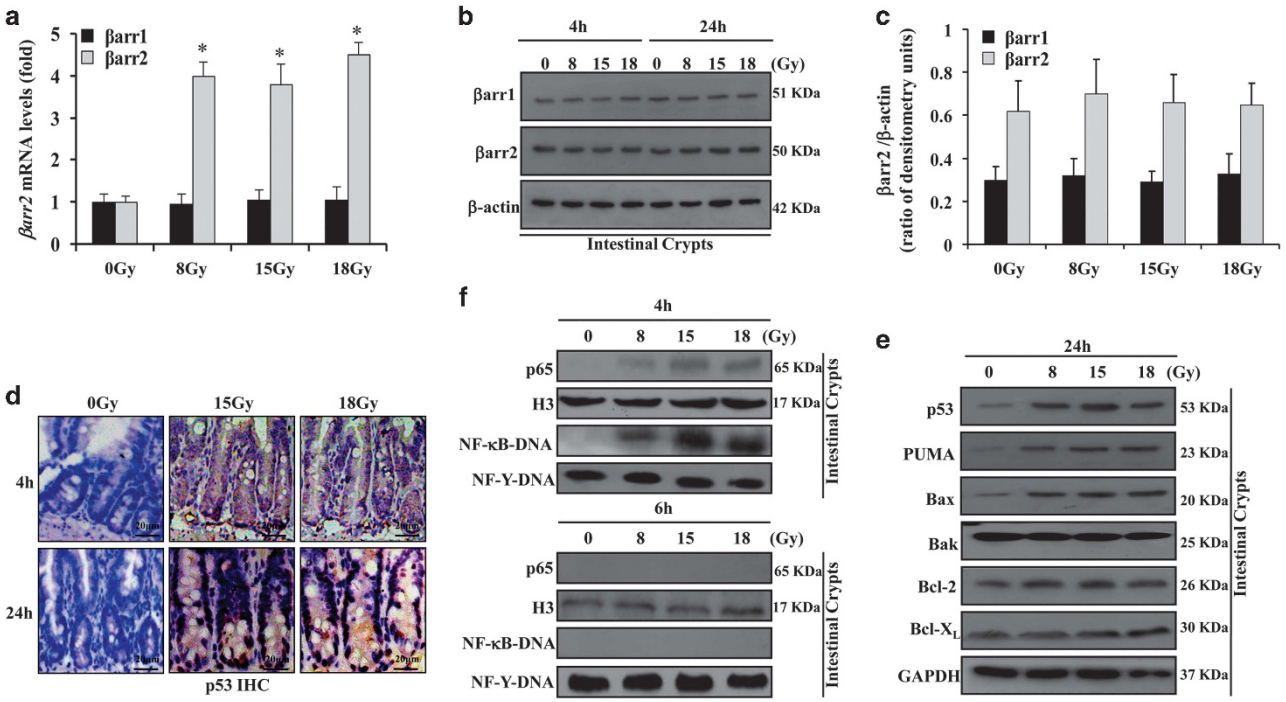

Figure 1 ICPS cell *β*arr expression and apoptosis-associated proteins in IR-treated mice. (**a**) *βarr* mRNA expression in ICPS cells of irradiated WT mice was determined by quantitative PCR at 24 h after IR. Values are means ± S.D., $n = 8$ in each group; $^*P < 0.001$ *versus* 0 Gy mice. (**b**) *β*Arr protein expression in ICPS cells of irradiated mice were evaluated by western blotting. *β*-Actin was used as the control for loading. (**c**) Quantifical analysis of western blotting of βarr expression in ICPS cells at 24 h after IR. (**d**) P53 expression in ICPS cells in WT mice was assessed by immunohistochemistry staining (brown) at 4 and 24 h after 15 and 18 Gy. (**e**) Proapoptotic protein p53, PUMA, Bax and Bak, and antiapoptotic protein Bcl-2 and Bcl-X_L, expression in isolated ICPS cells of irradiated mice were measured by western blotting. Glyceraldehyde 3-phosphate dehydrogenase (GAPDH) was used as the control for loading. (**f**) Western blotting analysis of nuclear translocation of NF-κB p65 and EMSA analysis of NF-κB DNA-binding activities in isolated ICPS cells of mice following IR. GAPDH, H3 and NF-Y-DNA complex was used as the control for loading

stem cells, mice with *Lgr5-eGFP* knock-in and *βarr2* KO (*Lgr5*/*βarr2* KO) were used. The total crypts in the longitudinal section of the small intestine had almost completely vanish at day 4 after IR at 15 Gy in *Lgr5*/*βarr2* WT mice, whereas 30 ± 5 crypts still remained in *Lgr5*/*βarr2* KO mice (Figures 3a and b). The average crypt depth of the small intestine in *Lgr5*/*βarr2* KO mice at day 2 after 15 Gy was 1.6-fold that in their WT counterparts (Figure 3c). The number of crypts was closely related to the number of surviving stem cells in the irradiated intestine. By quantifying intestinal stem cell variation using fluorescent staining (red) for the stem cell marker *Lgr5*-eGFP, we found that $Lgr5^+$ (leucine-rich repeat-containing G-protein-coupled receptor 5-positive) stem cells were reduced by more than 60% within 24 h and irradiated within 48 h after IR at 15 Gy in *Lgr5*/*βarr2* WT mice (Figures 3d and e). $Lgr5^+$ stem cell apoptosis following IR at 15 Gy decreased the total stem cells counted in 100 crypts by 22% in the first 24 h and by 18% on the second day in *Lgr5*/*βarr2* KO mice, compared with the level in *Lgr5*/*βarr2* WT mice (Figures 3d and e). These findings were further supported by stem cell double staining of Lgr5 and TUNEL (TdT-mediated dUTP nick-end labeling). In the first 24 h after IR at 15 Gy, *βarr2* deficiency reduced apoptotic $Lgr5^+$ stem cells by more than 80%, as observed in the *Lgr5*/*βarr2* WT mice (Figures 3f and g). The data above imply that βarr2 has an essential role in IR-induced intestinal stem cell apoptosis.

βArr2 did not contribute to IR-induced endothelial apoptosis in the intestine. Previous studies implicated vascular endothelial cell apoptosis in the initiation and development of GI syndrome.[7] However, we found that apoptosis induced by IR in the lamina propria of WT mice did not vary during 4 h following different doses of radiation (Figures 4a and b and Supplementary Figures 2c and f), and was consistently reduced by over 60% at 24 h (Figures 4a and b). Surprisingly, vascular endothelial cell apoptosis was not markedly influenced in *βarr2* KO mice. Using an endothelial marker, CD31, we discovered that a small proportion (20%) of CD31-positive cells suffered programmed cell death 4 h after IR at 18 or 15 Gy (Figures 4c and d and Supplementary Figures 2a, b, d and e), which was reduced to 8% at 24 h (data not shown). Nevertheless, neither the proportion of apoptotic CD31-positive cells nor the overall number of CD31-positive cells following IR significantly differed between *βarr2* WT and *βarr2* KO mice (Figures 4d and f and Supplementary Figures 2a and b). Furthermore, IR-induced endothelial cell apoptosis occurred in the first hour following IR at 15 Gy and evoked a remarkable decrease in these cell numbers within 4 h (Figure 4e and Supplementary Figure 2a). These results suggest that βarr2 is not required for vascular endothelial cell apoptosis in the villus following IR.

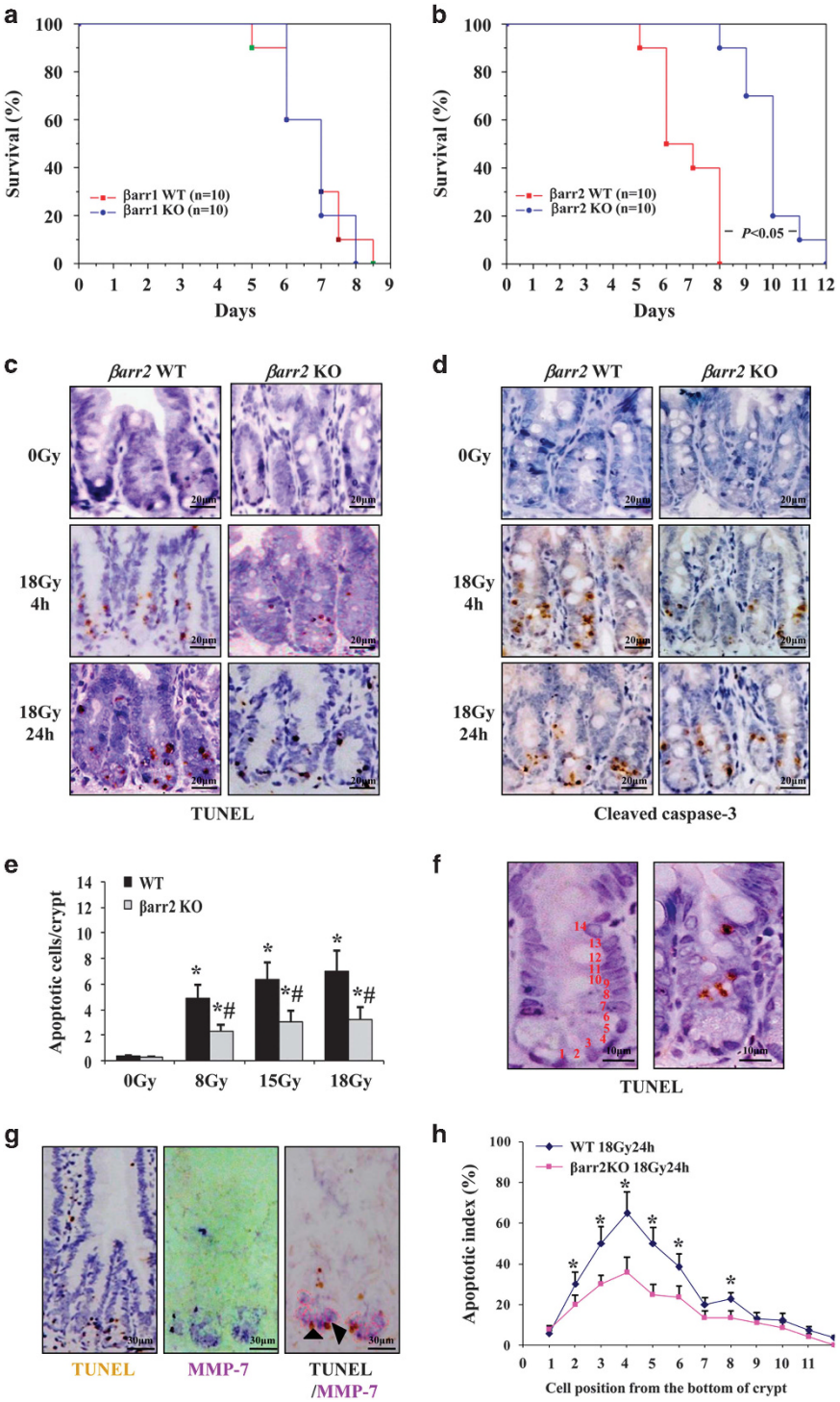

Figure 2 *βArr2* deficiency impaired IR-induced ICPS cell apoptosis. (**a** and **b**) Survival curves of mice subjected to 15 Gy. Three independent experiments were repeated. (**c**) Apoptosis in ICPS cells at 4 and 24 h after 18 Gy were analyzed by TUNEL staining (brown). (**d**) Caspase-3 activity in ICPS cells at 4 and 24 h after 18 Gy were evaluated by immunohistochemistry (brown). (**e**) Apoptotic index in ICPS cells at 24 h after IR measured by TUNEL staining. Values are means ± S.D., $n=8$ in each group; $^{*}P<0.01$ *versus* 0 Gy mice; $^{\#}P<0.05$ *versus* WT mice. (**f**) The representative example of apoptotic cells and their position in crypt in WT mice at 4 h following 18 Gy. (**g**) Radiation-induced apoptosis with triangle marked in the CBCs in WT mice. Sections were stained with TUNEL or TUNEL followed by MMP-7 IHC with several CBCs circled. (**h**) Apoptotic index at 24 h following 18 Gy. Each apoptotic index was scored as the mean percentage of apoptotic cells of each cell position, pooled from eight mice in each group; $^{*}P<0.05$, *versus* KO mice in each

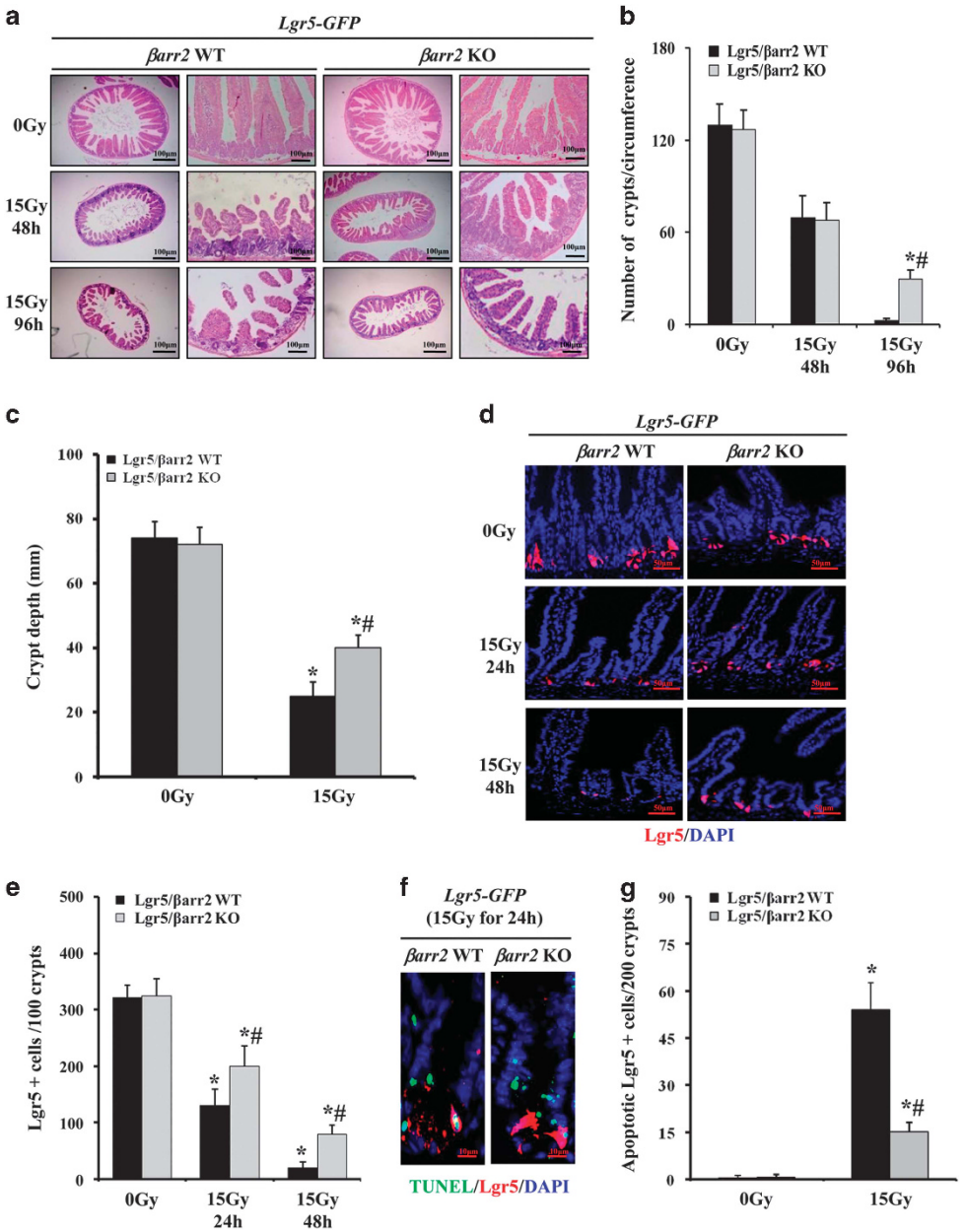

Figure 3 Targeted deletion of βarr2 attenuated intestinal Lgr5$^+$ stem cell apoptosis in response to IR. (**a**) Hematoxylin and eosin (HE) staining of small intestine sections. (**b**) The average number of small intestinal crypts in longitudinal section in indicated times after 15 Gy was assessed by counting surviving crypt. Values are means ± S.D., $n=8$ in each group; *$P<0.01$ *versus* 0 Gy mice; $^{\#}P<0.01$ *versus* WT mice. (**c**) Average depth of small intestinal crypt at 48 h after 15 Gy was measured. Values are means ± S.D., $n=8$ in each group; *$P<0.05$ *versus* 0 Gy mice; $^{\#}P<0.01$ *versus* WT mice. (**d**) Lgr5 of intestinal stem cells marker staining by fluorescent staining (red) in irradiated mice. The number of Lgr5$^+$ stem cells (red) was analyzed. (**e**) The average number of Lgr5$^+$ cells in the indicated times following 15 Gy was measured by counting fluorescent staining (red) in intact crypts. Values are means ± S.D., $n=8$ in each group; *$P<0.01$ *versus* 0 Gy mice; $^{\#}P<0.05$ *versus* WT mice. (**f**) Representative example of apoptotic Lgr5$^+$ cells or CBCs by fluorescent staining (red) and TUNEL staining (green). (**g**) Quantification of Lgr5$^+$ cells with TUNEL-positive signal in 200 intact crypt at 24 h following 15 Gy were analyzed. Values are means ± S.D., $n=8$ in each group; *$P<0.05$ *versus* 0 Gy mice; $^{\#}P<0.05$ *versus* WT mice

βArr2 regulated IR-induced NF-κB activation in ICPS cells. As IR has been confirmed to induce intestinal NF-κB activation,[15,16,26] we first detected whether *β*arr2 has a role in IR-induced intestinal NF-κB activation. Twenty-four hours after the irradiation of WT mice at 15 Gy, IκB*α* degradation occurred in ICPS cells, which was much more extensive than that in *βarr2* KO mice (Figure 5a). Next, IR-evoked NF-κB activity-related events following IκB*α* degradation were investigated. The nuclear translocation of NF-κB p65 and NF-κB DNA-binding activity were promoted within 12 h and had completely disappeared at 24 h after IR at 15 Gy in ICPS cells of *βarr2* KO mice (Figure 5a), which were transiently activated within 4 h and had vanished by 6 h after IR at 15 Gy in ICPS cells of WT mice (Figures 5a and b). Previous results showed that the apoptotic index in intestinal crypts was lower in *βarr2* KO mice compared with that in WT mice following IR

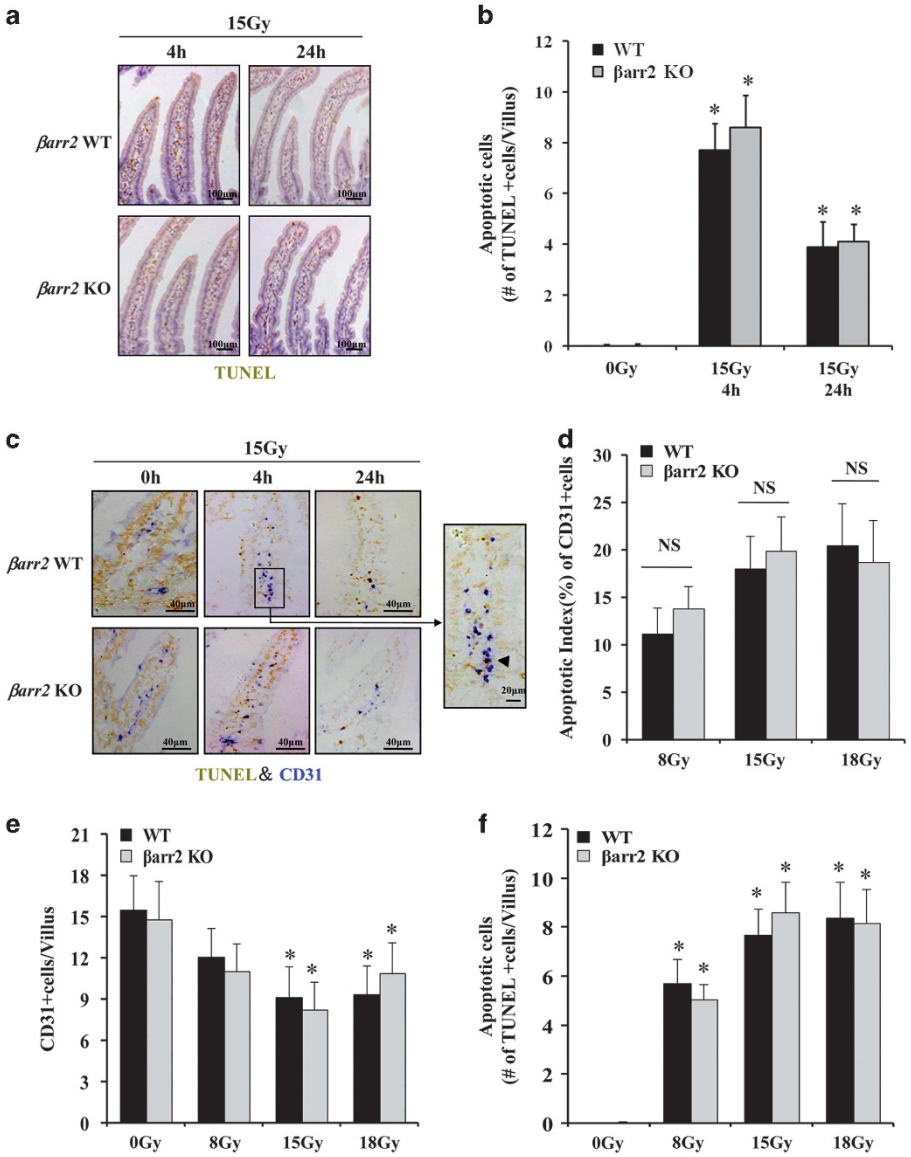

Figure 4 βArr2 did not contribute to IR-induced endothelial apoptosis in the intestine. (**a**) Apoptosis induced by radiation in villus was evaluated by TUNEL staining (brown). (**b**) The average apoptotic index in villus submucosa at 4 and 24 h after 15 Gy was scored by TUNEL staining (brown). Values are means ± S.D., $n = 8$ mice in each group; *$P < 0.05$ *versus* 0 Gy mice. (**c**) The sections were double stained with TUNEL (brown) and CD31 (blue). Arrow indicate double-positive cell. (**d**) The average fraction (%) of $TUNEL^+/CD31^+$ cells in the villus at 4 h after IR. Values are means ± S.D., $n = 8$ mice in each group. NS, no significance. (**e**) The average number of $CD31^+$ cells in villus submucosa at 4 h after IR. Values are means ± S.D., $n = 8$ mice in each group; *$P < 0.05$ *versus* 0 Gy mice. (**f**) The average apoptotic index in villus submucosa at 4 h after IR. Values are means ± S.D., $n = 8$ mice in each group; *$P < 0.05$ *versus* 0 Gy mice

(Figures 2a and c). Intriguingly, the lower apoptotic index in ICPS cells of *βarr2* KO mice, compared with those in WT mice was compromised by intraperitoneal injection of the NF-κB inhibitor Bay117082 (Figures 5b, d and e). The NF-κB inhibitor Bay117082 significantly upregulated PUMA expression (Figure 5b), but had little impact on IR-induced endothelial cell apoptosis (data not shown). These results strongly suggest that βarr2 restricts IR-induced NF-κB activation in ICPS cells.

***βArr2* KO suppressed IR-induced ICPS cell apoptosis via the PUMA-mediated mitochondrial pathway.** IR has been shown to cause mitochondrial dysfunction.[27] To investigate the effect of βarr2 on IR-induced mitochondrial injury, we analyzed mitochondrion-related events in ICPS cells. We found that IR caused cytosolic release of cytochrome *c* and its mitochondrial translocation in ICPS cells of WT mice, whereas these were almost completely suppressed in ICPS cells of *βarr2* KO mice (Figure 6a). Nevertheless, IR induced PUMA expression, and caspase-9 and -3 activities, which were significantly inhibited in ICPS cells of *βarr2* KO mice (Figure 6b). PUMA-mediated mitochondrial apoptosis has been shown to be a crucial factor for IR-evoked intestinal apoptosis.[28] To further confirm that βarr2 is involved

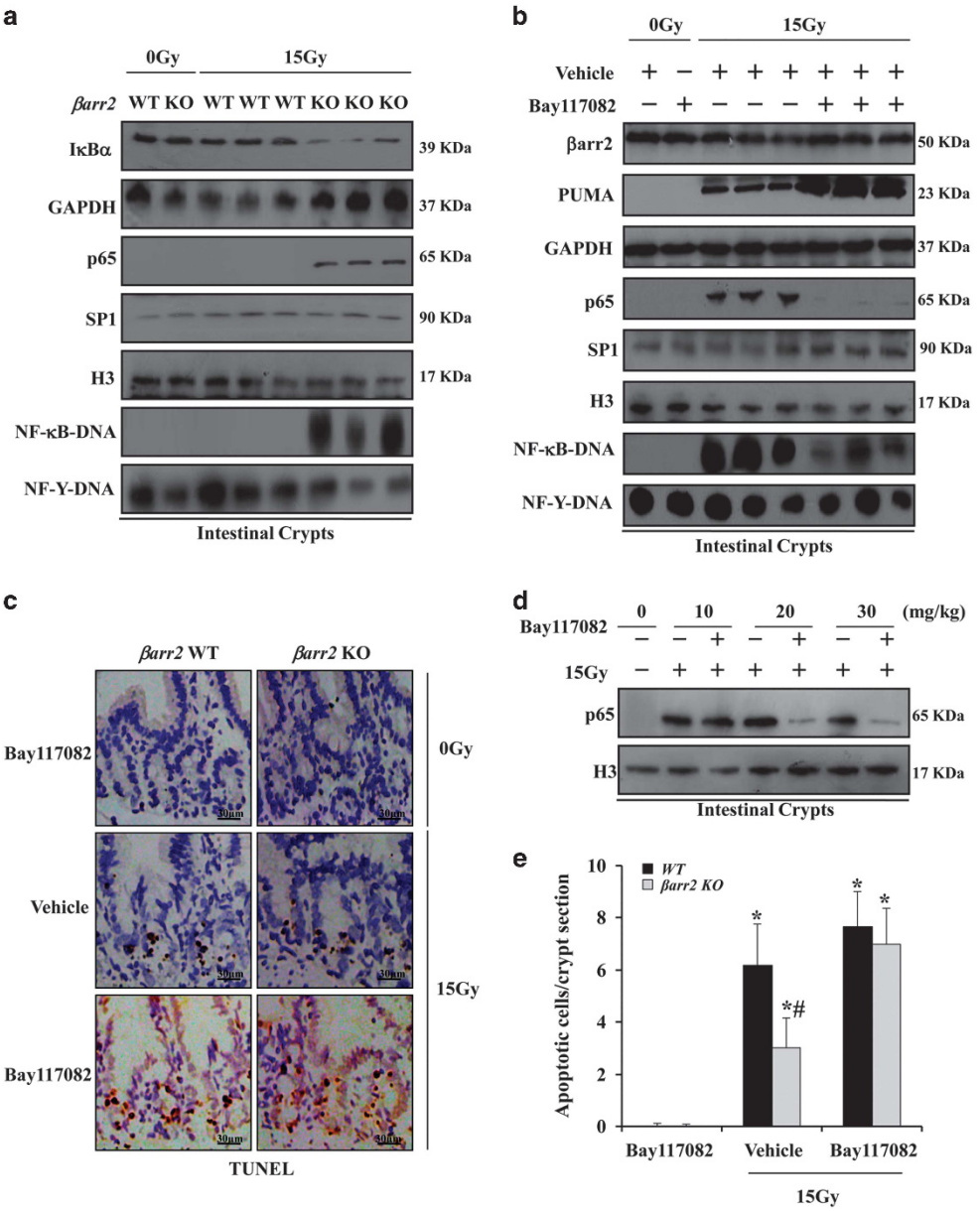

Figure 5 βArr2 regulated IR-induced NF-κB activation in ICPS cells. (**a**) Western blotting analysis of IκBα, nuclear translocation of NF-κB p65 and EMSA analysis of NF-κB DNA-binding activities in ICPS cells from mice at 12 h after 15 Gy. Glyceraldehyde 3-phosphate dehydrogenase (GAPDH), H3 and NF-Y-DNA complex was used as the control for loading. (**b**) Western blotting analysis of βarr2 and nuclear translocation of NF-κB p65 and EMSA analysis of NF-κB DNA-binding activities in ICPS cells from mice at 4 h after 15 Gy. GAPDH, H3 and NF-Y-DNA complex was used as the control for loading. (**c**) Apoptosis in ICPS cells at 24 h after 15 Gy were observed by TUNEL staining (brown). (**d**) Western blotting analysis of nuclear translocation of NF-κB p65 in ICPS cells from mice with or with not pretreatment of the indicated doses of Bay117082 at 4 h after 15 Gy. (**e**) Apoptotic index in ICPS cells was calculated by TUNEL staining (brown) at 24 h after 15 Gy. Values are means ± S.D., $n = 8$ in each group; $^{*}P < 0.01$ *versus* Bay117082-treated mice; $^{\#}P < 0.005$ *versus* WT mice

upstream of PUMA-mediated mitochondrial dysfunction, we used *PUMA* KO mice exposed to IR at 15 Gy and found that compared with *PUMA* WT mice, the cryptic apoptotic index was markedly decreased in *PUMA* KO mice (Figures 6c and d), which is consistent with previous findings.[28] Moreover, βarr2 expression, nuclear translocation of nuclear p65 and NF-κB DNA-binding activity in ICPS cells did not significantly vary between *PUMA* WT and KO mice following IR at 15 Gy (Figure 6e), but the NF-κB inhibitor Bay117082 significantly promoted PUMA expression (Figure 5b). These results indicate that βarr2, through NF-κB, regulates PUMA-mediated mitochondrial apoptosis caused by IR in ICPS cells of mice.

βArr2 regulated IR-induced cell apoptosis through NF-κB/PUMA signaling in HCT116 cells and Lgr5^{+} cells. To elucidate the mechanism by which βarr2 regulates PUMA expression in IR-induced apoptosis, we tested the effect of

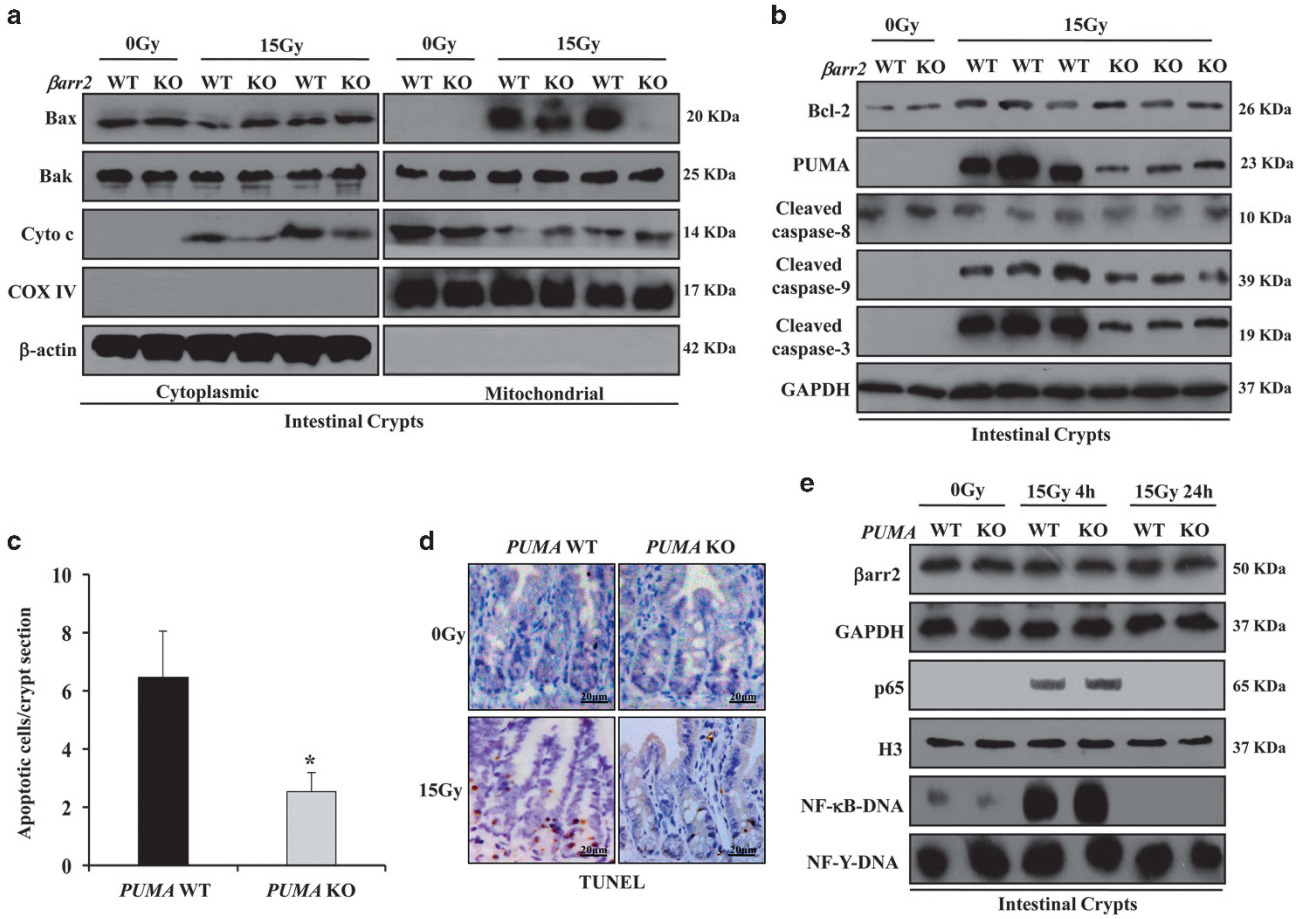

Figure 6 *βArr2* KO suppressed IR-induced ICPS cell apoptosis via the PUMA-mediated mitochondrial pathway. (**a**) Bax, BaK and Cyto C were analyzed in the cytosolic and mitochondrial fractions of ICPS cells from mice at 24 h after 15 Gy by western blotting. *β*-Actin and cycloxygenase IV (COX IV) were used as the controls for loading and fractionation. (**b**) Bcl-2, PUMA, cleaved caspase-3, -8 and -9 levels were evaluated in ICPS cells from mice at 24 h after 15 Gy by western blotting. Glyceraldehyde 3-phosphate dehydrogenase (GAPDH) was used as the controls for loading. (**c**) Apoptosis in ICPS cells at 24 h after 15 Gy were observed by TUNEL staining (brown). (**d**) Apoptotic index in ICPS cells scored by TUNEL staining (brown) at 24 h after 15 Gy. Values are means ± S.D., $n = 8$ in each group. (**e**) Western blotting analysis of *β*arr2 and nuclear translocation of NF-*κ*B p65 and EMSA analysis of NF-*κ*B DNA-binding activities in ICPS cells from mice at 4 and 24 h after 15 Gy. GAPDH, H3 and NF-Y-DNA complex was used as the control for loading

downregulating βarr2 expression and NF-*κ*B activation on IR-induced apoptosis in HCT116 cells treated with *β*arr2 siRNA and the NF-*κ*B inhibitor Bay117082, respectively, before IR at 20 Gy. We found that apoptosis was markedly mitigated in cells with *β*arr2 RNA interference compared with cells with vector treatment (Figures 7a–c). Moreover, we also found that βarr2 had interacted and colocalized with IB*κα*, a key kinase of the NF-*κ*B pathway, and that IB*κα* could be suppressed by *β*arr2 RNA interference following IR (Figures 7d–f). This explains the marked activation of nuclear translocation of NF-*κ*B p65 and NF-*κ*B DNA-binding activity in cells with *β*arr2 RNA interference compared with those in cells with vector treatment (Figure 7f). At the same time, βarr2 knockdown restrained Bax translocation into the mitochondria and caspase-3 activity, but left Bcl-2 expression unchanged (Figures 7g and h). In contrast, the NF-*κ*B inhibitor Bay117082 at a concentration of 30*μ*M, optimized by intranuclear p65 detection (Supplementary Figure 3a) and the 3-(4,5-dimethylthiazol-2-yl)-2,5-diphenyltetrazolium) bromide (MTT) method (data not shown), significantly increased cell apoptosis and blocked IR-stimulated NF-*κ*B activation following IR at 20 Gy (Supplementary Figures 3b–e). In addition, Bay117082 increased Bax translocation and caspase-3 activity. However, unexpectedly, it did not alter Bcl-2 expression (Supplementary Figure 3e). More importantly, PUMA expression was downregulated in cells pretreated with *β*arr2 RNA interference, but was upregulated in those subjected to Bay117082 treatment (Figure 7f and Supplementary Figure 3f).

To further confirm the role of βarr2 in radiation-induced stem cell apoptosis, $Lgr5^+$ cells, known as intestinal stem cells, were isolated and cultured (Supplementary Figures 4a and b). We found that βarr2 protein expression was greatly elevated at 4 and 24 h after IR at three doses, but βarr1 protein expression was not apparently changed by IR in $Lgr5^+$ cells (Supplementary Figures 4c). With the inhibition of βarr2 expression, the apoptotic index of $Lgr5^+$ cells following IR was significantly reduced (Supplementary Figures 4d). Next, we found that βarr2 interacted with IB*κα*, and that IB*κα* could be repressed by *β*arr2 RNA interference following IR

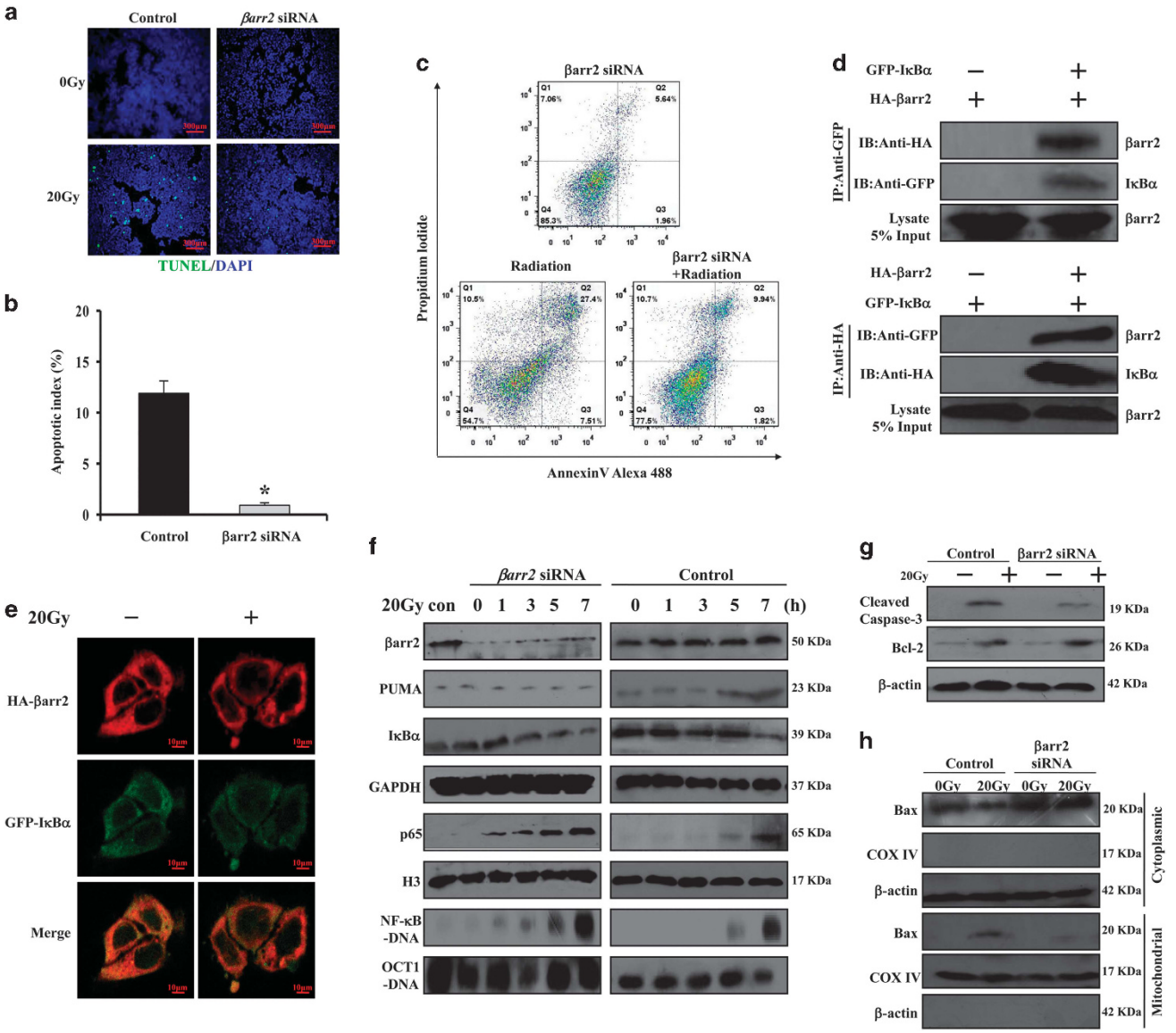

Figure 7 βArr2 regulated IR-induced cell apoptosis through NF-κB/PUMA signaling in HCT116 cells and Lgr5$^+$ cells. (**a**) TUNEL analysis at 24 h after 20 Gy of HCT116 cultured cells pretreated with βarr2 siRNA for 48 h before insult by 20 Gy. (**b**) The apoptotic index at 24 h after 20 Gy was calculated by counting a minimum of 20 randomly selected ×200 microscopy fields following TUNEL staining. The index was obtained by dividing the TUNEL-positive cells by the total number of cells. Three independent experiments were repeated, $^*P<0.01$. (**c**) Flow cytometry analysis for Annexin V-positive cells in cultured cells pretreated with βarr2 RNA interference for 48 h before radiation treatment at 24 h following 20 Gy. (**d**) βArr2 and IBκα were expressed together in cells. Proteins immunoprecipated with green fluorescence protein (GFP) or hemagglutinin (HA)-specific antibody or cell lysate were subject to immnoblotting with antibody against HA or GFP as indicated. (**e**) Colocalization of HA-βarr2 and GFP-IBκα in HCT116 cells at 24 h after 20 Gy. HA-βarr2 (red) and GFP-IBκα (green) were detected with HA or GFP antibody. (**f**) βArr2, IκBα, nuclear protein p65 and H3 expression in HCT116 cells with or without βarr2 siRNA were detected at the indicated times after 20 Gy by western blotting. NF-κB DNA-binding activity was measured βy EMSA. GAPDH, H3 and OCT1-DNA complex was used as the control for loading. (**g**) Caspase-3 activity and Bcl-2 in HCT116 with or with not βarr2 siRNA were quantified by western blotting at 24 h after 20 Gy. (**h**) Bax was analyzed in the cytosolic and mitochondrial fractions of HCT116 cells at 24 h after 20 Gy with or without βarr2 siRNA. β-Actin and cycloxygenase IV (COX IV) were used as the controls for loading and fractionation

(Supplementary Figures 4e and f). Consequently, the nuclear translocation of NF-κB p65 was distinctly activated in Lgr5$^+$ cells with βarr2 RNA interference following IR. These findings further support the claim that βarr2 potentiates IR-stimulated intestinal stem cell apoptosis by regulating the NF-κB/PUMA pathway.

***βArr2* deficiency prolonged the survival of mice following abdominal irradiation.** The cause of mortality in mice upon exposure to radiation at doses of more than 14 Gy is GI syndrome not bone marrow aplasia.[2] GI syndrome is believed to be important for decreasing the number of intestinal progenitor/stem cells in response to lethal radiation. Therefore, we speculated that enhancing progenitor/stem cell survival in *βarr2* KO mice would result in increased crypt proliferation and regeneration following IR. A comparison of cryptic cell reproduction in *βarr2* WT and KO mice revealed significant differences in 24 h after 15 Gy. The number of

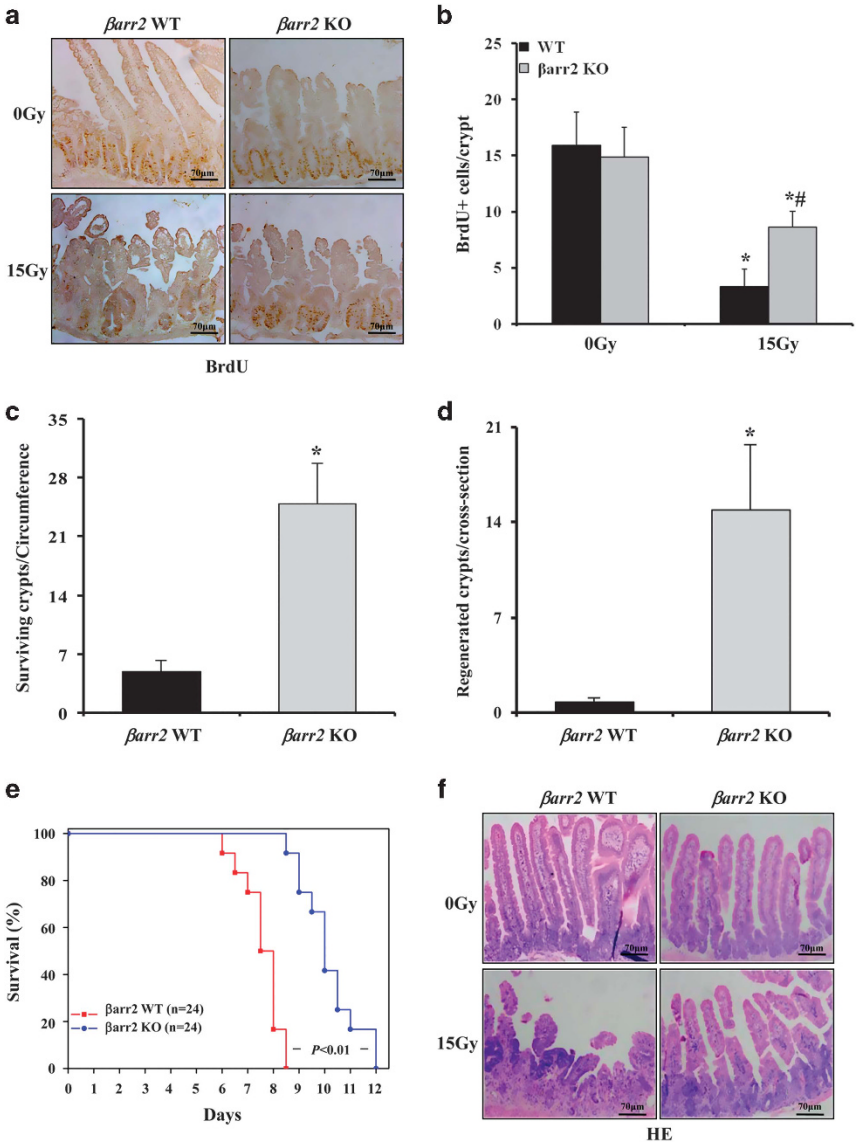

Figure 8 *βArr2* deficiency prolonged the survival of mice following abdominal irradiation. (**a**) Bromodeoxyuridine (BrdU) staining at 24 h after 15 Gy of small intestine sections. (**b**) BrdU incorporation index in small intestine at 24 h after 15 Gy was quantitated by counting 100 intact crypts. Values are means ± S.D., $n = 8$ mice in each group; $^{*}P < 0.05$ *versus* 0 Gy mice; $^{\#}P < 0.01$ *versus* WT mice. (**c**) Surviving crypt was counted in longitudinal section and crypt regeneration was calculated by counting 10 cross-sections following BrdU staining at day 4 after 15 Gy. Values are means ± S.D., $n = 8$ in each group; $^{*}P < 0.01$. (**d**) Crypt regeneration was calculated by counting 10 cross-sections following BrdU staining at day 4 after 15 Gy. Values are means ± S.D., $n = 8$ in each group; $^{*}P < 0.05$. (**e**) Survival curves of mice subjected to 15 Gy. (**f**) Hwmatoxylin and eosin (HE) staining of small intestine sections at day 4 after 15 Gy

BrdU-positive cells per crypt 24 h after IR at 15 Gy in *βarr2* KO mice was two times as that in WT mice (Figures 8a and b). Microcolony assay was performed to detect the regenerative capacity of stem cells at day 4 after IR at 15 and 18 Gy. We found that the number of regenerated crypts in *βarr2* KO mice was significantly greater than that in WT mice (Figures 8c and d and Supplementary Figures 5a, b and e). The intestinal epithelium was completely restored in both WT and *βarr2* KO mice by 4 days after IR at 8 Gy (Supplementary Figure 5d).

Next, we investigated whether the disparities in crypt apoptosis and regeneration in irradiated WT and *βarr2* KO mice affected their survival. *βArr2* KO mice were shown to survive longer than their WT counterparts after IR at 15 Gy (Figure 8e). Histological analysis was then used to uncover marked differences in the extent of intestinal injury. A progressive decline in the length of villi and gradual denudation of the epithelium were recorded in WT mice 4 days after IR at 15 and 18 Gy (Figure 8f and Supplementary Figure 5c). Thickening of the lamina propria and extensive infiltration of inflammatory-related cells into the submucosa suggested intestinal mucosal unintegrity (Figure 8f). However, the degradation of villi, mucosal inflammatory response and irregular architecture in the lamina propria were significantly attenuated in *βarr2* KO mice (Figure 8f). This could explain the observation that 50% of WT mice had died, whereas 100% of

βarr2 KO mice were still alive, 7 days after IR at 15 Gy (Figure 8e). These findings suggest that βarr2 has a crucial impact on the development of GI syndrome and the death of cologenic stem cells following lethal doses of IR.

Discussion

In our study, *βarr2* deficiency postponed GI syndrome and prolonged the survival of mice subjected to lethal doses of IR. To our knowledge, few studies have focused on a single protein whose manipulation significantly regulates GI syndrome via securing stem cell zones and the integrity of intestinal epithelium.[29] Importantly, with the aid of a defined intestinal stem cell marker, Lgr5, and a mouse model,[5] we also found that, compared with their WT counterparts, intestinal Lgr5$^+$ stem cells with *βarr2* deficiency in the crypt base were more radioresistant (Figures 2 and 3) and subsequently improved crypt reproduction.

Our findings have several important implications. First, *Lgr5* mice provide explicit evidence that intestinal stem cell damage is the pivotal factor behind GI syndrome (Figure 3).[6,28] Second, our experiment indicates that the genetic ablation of βarr2 comprehensively prevented intestinal crypt cell apoptosis within 24 h (Figure 2), although IR had little effect on the induction of βarr2. βArr2 protein was not induced by radiation in intestinal crypts. This is because that Lgr5$^+$ cells just account for very small number of cells in crypt cell population and the alteration of βarr2 protein expressed in Lgr5$^+$ cells was masked by the expression of other cell population in crypts. With isolation of Lgr5$^+$ cells from intestinal crypts, we found that three doses of radiation significantly induced βarr2 protein expression in Lgr5$^+$ cells (Supplementary Figure 4). All these explain the results of cell proliferation and survival analysis showing that *βarr2* deficiency elevated crypt proliferation and regeneration and preserved the intestinal architecture and integrity at a later phase (Figure 8). In contrast, βarr2 ablation had little effect on IR-induced apoptosis of vascular endothelial cells (Figure 4). Thus, intestinal ICPS cell apoptosis is the critical factor behind GI syndrome following IR, which is consistent with other studies.[2] Furthermore, our observations do not support the model that switches damage from the villus endothelium to crypt progenitor/stem cells in irradiated intestine,[7,8,30] because the apoptosis of vascular endothelial cells markedly decreased within 24 h and was unchanged by IR at 15 and 18 Gy. The disparity between our findings and these previous results might be partly attributable to the different strains of mice and different endothelial cell markers used. Consequently, our data suggest that ICPS cell apoptosis dominant over villus vascular endothelial cell apoptosis in the initiation of IR-induced GI syndrome.

Previous studies have shown that NF-*κ*B activation defends some cancer cells against the cytotoxicity of IR;[31] conversely, IKK*β*-deficient mice with defective activation of the NF-*κ*B canonical pathway were more radiosensitive in the small intestine and exhibited lower survival following IR.[14] Our results indicate that prolonged NF-*κ*B activation in ICPS cells of βarr2 KO mice in the first 24 h after IR markedly promoted ICPS survival at 48 h after IR, which explains the superior survival of βarr2 KO mice, and the inhibition of NF-*κ*B activation with a chemical agent markedly escalated IR-induced ICPS cell apoptosis. More importantly, we found that NF-*κ*B-mediated intestinal radioprotection was the main player in the suppression of PUMA. PUMA has been shown to be a crucial mediator of intestinal apoptosis.[28] NF-*κ*B activation by IR encouraged ICPS cell survival by inhibiting PUMA-mediated mitochondrial apoptosis (Figure 7). Our findings also indicated that *βarr2* deficiency with much stronger and protracted IR-evoked NF-*κ*B activation markedly downregulated PUMA induction, but hardly altered Bcl-2 expression, which is the target gene of NF-*κ*B (Figures 6b and 7). Future work is thus clearly needed to address the small effect of the βarr2/NF-*κ*B pathway on Bcl-2 induction by IR.

Past researches have shown that IR insult in the intestinal epithelium primarily induces three signal pathways, namely the p53, JNK and NF-*κ*B pathways.[14,32–35] In the small intestine of irradiated mice, whereas the activation of p53 and JNK is proapoptotic,[32–35] the activation of NF-*κ*B functions as an antiapoptotic signal.[14] It is widely believed that IR-induced GI syndrome is closely associated with an imbalance between pro- and antiapoptotic functions of these signal pathways in ICPS cells. The current study provides direct evidence for the targeting of βarr2 to promote and prolong antiapoptotic NF-*κ*B activation, rebalance proapoptotic and antiapoptotic signal pathways and thereby diminish ICPS cell apoptosis induced by IR. The effective suppression of IR-induced NF-*κ*B activation by βarr2 reveals that in the future, small-molecule βarr2 inhibitors with desirable pharmacological properties might be useful for the prevention and management of IR-induced GI syndrome.

Materials and Methods

Mice and IR. All animal experiments were approved by the Institutional Animal Care and Use Committee at Sun Yat-sen University (Guangzhou, China). C57/BL6 *βarrs* (*βarr1* and *βarr2*) heterozygotes were generously donated by Dr. Robert J Lefkowitz (Duke University Medical Center, Durham, NC, USA). *Lgr5-GFP* knock-in mice (*Lgr5*$^+$ mice)[5] and *PUMA* KO mice were purchased from The Jackson Laboratory (Bar Harbor, ME, USA). Eight- to 10-week-old *βarrs* wild-type (WT) and *βarrs* KO littermates were generated by C57BL/6 *βarr2* heterozygote breeding. Previously described *Lgr5 (Lgr5-GFP)* mice were crossed with *βarr2* KO mice to generate *Lgr5/βarr2* WT and *Lgr5/βarr2* KO mice. The mice were housed and genotyped as described previously.[36] Mouse (25–30 g) with head, thorax and the legs shielded by plumbum were abdominally irradiated at doses of 8, 15 and 18 Gy at a rate of 2 Gy/min using an RS-2000 X-ray Biological Irradiator (RAD Source Technologies, Suwanee, GA, USA). To minimize the effect of genetic background, for every experiment age-matched, littermate controls were used. Therefore, potential genetic modifiers of the response to radiation would be randomly distributed among the experimental and control groups.

Isolation of ICPS cells. The crypt progenitor/stem cells of the small intestinal were isolated as described previously.[5,37] Briefly, small intestines were opened longitudinally, cut into 5-mm pieces and incubated in 2 mM ethylenediaminetraacetic acid (EDTA) with phosphate-buffered saline (PBS) at 37 °C for 30 min. After removal of the EDTA medium, the samples were vigorously suspended using a 10-ml pipette with PBS. The supernatant was the villous fraction and was removed; the sediment was then resuspended with PBS. After further vigorous suspension and centrifugation, the supernatant was enriched for crypts. This fraction was passed through a 70-mm cell strainer (BD Bioscience, Franklin Lake, NJ, USA) to remove residual villous material. Isolated crypts were centrifuged at 150–200 × *g* for 3 min to separate crypts from single cells. The final fraction consisted of essentially pure crypts for the extraction of total proteins and nuclear proteins.

Isolation, culturing and transfection of Lgr5$^+$ cells. The intestinal cells were isolated from Lgr5-EGFP-IRES-creERT2 mice as described previously.[38] The proximal intestinal segment (jejunum) was cut open at 1 cm longitudinally in a

tissue culture dish, incubated in PBS containing 30 mM EDTA and 1.5 mM DL-dithiothreitol (Sigma-Aldrich, St. Louis, MO, USA) on ice for 20 min and transferred to a 15 ml conical tube containing 5 ml of 30 mM EDTA in PBS. The tube with the tissue was incubated at 37 °C for 8 min, and then shaken by hand for 30 s at three shake cycles per second. After shaking, the remnant muscle layer was removed, and the dissociated cells were pelleted at 800 × *g*, resuspended in PBS+10% fetal bovine serum (FBS) and repelleted at 400 × *g*. The cells were then incubated in 10 ml of modified Hank's buffered salt solution (mHBSS) containing 0.3 U/ml dispase (BD Biosciences, Bedford, MA, USA) at 37 °C for 10 min with intermittent shaking every 2 min for 30 s to separate epithelial sheets into single cells. The cell suspension was then supplemented with 1 ml of FBS and 1000 U DNase (AppliChem, St. Louis, MO, USA) and then sequentially passed through 70 and 40 μM filters (BD Biosciences). Cells were pelleted and resuspended in 10 ml of HBSS and then repelleted and resuspended at a concentration of 2×10^7 cells per ml in intestinal epithelial stem cell (IESC) medium (Advanced DMEM/F12 supplemented with 1 × N2, 1 × B27, 10 mM HEPES, 10 μM Y27632, 100 μg/ml penicillin/streptomycin). Approximately 1×10^7 cells were incubated in IESC medium with antibodies (α-CD31-PE/Cy7, α-CD45-PE/Cy7 and PI) on ice for 30 min with mixing every 10 min. The CD31/CD45/PI triple-negative population was sorted as total intestinal epithelial cells, and the Lgr5-eGFP high fraction, 10 000 cells each.

The $Lgr5^+$ cells were routinely cultured in IESC medium (Advanced DMEM/F12 supplemented with 1 × N2, 1 × B27, 10 mM HEPES, 10 μM Y27632, 100 μg/ml penicillin/streptomycin) supplemented with 10% FBS at 37 °C under 5% CO_2.

The $Lgr5^+$ cells were transfected by LipofectAMINE (Invitrogen, Carlsbad, CA, USA). Full-length IκBα was cloned into modified pcDNA3 vector in-frame with Flag at the N terminus and full-length βarr2 was cloned into modified pcDNA3 vector in-frame with HA at the C terminus.[39] The transfection was performed according to the manufacturer's instruction. First, the cells were transfected in 80–90% density. Lipofectamine was diluted in Opti-MEM (Invitrogen) medium and DNA was diluted in Opti-MEM medium. Afterwards, diluted DNA was added to diluted Lipofectamine for 10 min incubation at room temperature. Finally, DNA-Lipo complex was added to cells and incubated for 24 h. Western blotting was used to verify the efficiency and effectiveness of transfection.

HCT116 cell culture, βarr2 RNA interference, apoptosis evaluation and MTT. HCT116 human colon cancer cells were cultured in complete medium consisting of DMEM/F12 (Thermo Fisher Scientific, Waltham, MA, USA) supplemented with 10% FBS at 37 °C in a CO_2 incubator and exposed to 20 Gy at a rate of 5 Gy/min using an RS-2000 X-ray irradiator (Rad Source Technologies). βArr2 knockdown was achieved by using βarr2 siRNA (Santa Cruz Biotechnology, Santa Cruz, CA, USA) in accordance with the manufacturer's instructions. The mixture, containing Lipofectamine (Invitrogen) and βarr2 siRNA dissolved in Optimal (Invitrogen), was added to cells at 80% confluence, and 48 h after interference, the cells were exposed to 20 Gy and harvested. Fluorescein-conjugated control siRNA was used to indicate successful transfection into cells.

Cell apoptosis was evaluated using an *In Situ* Cell Death Detection Kit (Roche, Basel, Switzerland) and an Annexin-V-Alexa Kit (Roche, Basel, Switzerland), respectively, according to the manufacturer's instruction. The apoptotic index was determined by TUNEL staining using a microscope and dividing the number of apoptotic cells by the total number of cells in a glass slide for at least 20 randomly selected fields (×200). With the Annexin-V-Alexa Kit, cell apoptosis was analyzed with a Canto II flow cytometer (Becton Dickinson, San Jose, CA, USA). Six independent experiments were repeated.

The evaluation of cytotoxicity for Bay117082 (Sigma Chemical Co., St. Louis, MO, USA) treatment was performed using the MTT assay. HCT116 cells were seeded at a density of 5000 cells per well in 96-well plates. Each well contained 100 μl of DMEM-F12 medium supplemented with 10% FBS, and the HCT116 cells were cultured for 24 h at 37 °C. The cells were then incubated with different concentrations of Bay117082 (0, 5, 10, 20 and 30 μM). After incubation, the medium was replaced with 100 μl of complete medium, and 10 μl of MTT solution (5 mg/ml) in PBS was added to each well. After the cells had been further incubated for 4 h, the MTT-containing medium was removed, and 110 μl of dimethylsulfoxide was added to each well. After the cells had been gently agitated for 5 min, the absorbance of each well was recorded with an Infinite F200 Multimode Plate Reader (Tecan, Crailsheim, Germany) at 490 nM. All experiments were conducted in triplicate. The data are represented as the mean ± S.D.

Histological analysis, TUNEL and BrdU staining. Some mice were injected with BrdU (150 mg/kg; Sigma Chemical Co.) 4 h before killing. Sections (3 μm thick) from paraffin-embedded intestinal bundles (jejunum) were subjected to hematoxylin and eosin staining for histological analysis.

TUNEL staining was carried out using an *In Situ* Cell Death Detection Kit (Roche), according to the manufacturer's instructions. The apoptotic index was determined in full longitudinal sections of intact crypt containing at least 14 cells, including Paneth cells. The average frequency of apoptosis for each cell position from the crypt bottom was scored in 200 half-crypt sections. Following BrdU staining, the average number of BrdU-positive cells in the crypt was scored by counting 100 intact crypts. The data are presented as mean ± S.D. Eight mice were used in each group. More details of the experimental procedures are described in the Supplementary Data. Three independent observers blinded to the genotype and treatment was responsible for apoptotic and proliferative index scoring.

Immunohistochemistry. The detailed methods for the staining cleaved caspase-3, MMP-7 and Lgr5 and double staining TUNEL/Lgr5 and pTUNEL/MMP-7 are described in the Supplementary Data.

Antibodies, western blotting, immunoprecipitation, immunofluorescence microscopy, nuclear and mitochondrial extraction, and EMSA. The methods and reagents used for these approaches are provided in the Supplementary Materials and methods. To detect Bax and cytochrome *c* translocation, intestinal mucosal samples were used to isolate mitochondrial and cytosolic fractions by the differential centrifugation method as described previously.[40] Electrophoretic mobility shift assay (EMSA) was performed using the LightShift Chemiluminescent EMSA Kit (Thermo Fisher Scientific) as described previously,[41] according to manufacturer's instructions. All experiments were conducted in triplicate.

Crypt microcolony assay. Stem cell survival was quantified by counting regenerated crypts in hematoxylin- and eosin-stained and BrdU-stained cross-sections 4 days after radiation[42–44] as detailed in the Supplementary Data. Surviving crypts were defined as those containing five or more adjacent chromophilic non-Paneth cells, at least one Paneth cell and a lumen. The regenerated crypts contained five or more BrdU-positive cells with a lumen. Eight mice were used in each group, and the data are presented as mean ± S.D.

Bay117082 treatment. Mice were injected intraperitoneally with an optimal dose of 20 mg/kg Bay117082 (Sigma Chemical Co.), an NF-κB inhibitor delivered 3 h before radiation. HCT116 cells were pretreated with optimal dose of 30 μmol/l Bay117082 1 h before radiation.

Total RNA extraction and real-time PCR. Total RNA was extracted from the intestinal mucosal scraping samples using the RNAgents Total RNA Isolation System (Promega, Madison, WI, USA) according to the manufacturer's instructions. cDNA was synthesized using Superscript Reverse Transcriptase (Invitrogen) according to the manufacturer's instructions. Real-time PCR was performed on an ABI7500 (Life Technology, Carlsbad, CA, USA) using gene-specific primers and DyNAmo SYBR Green Master Mix. *βarr2* was amplified using primers (Invitrogen). As an internal control, the expression of *β-actin* in each sample was also quantified using the sense primers (Invitrogen). Eight mice were used in each group.

Statistical analysis. All experiments were performed at least in triplicate. Results are expressed as mean ± S.D. and were analyzed by unpaired *t*-test or ANOVA; multiple comparisons were carried out using the method of least significant difference. Data in Figures 8e and d and Supplementary Figure S8E were also analyzed using the Mann–Whitney test, with the largest *P*-value depicted. The survival data were evaluated using log-rank test with the SPSS 17.0 software (IBM Corp., Armonk, NY, USA). Differences were considered significant if the probability of the difference occurring by chance was < 0.05 ($P < 0.05$).

Conflict of Interest

The authors declare no conflict of interest.

Acknowledgements. We are grateful to Professor Robert J Lefkowitz at Duke University for providing the β-arrestins KO mice and the β-arrestins antibody. We also thank Professor Xiuqing Wei, Dr. Weigang Dai, Dr. Yunjiu Cheng at Sun Yat-sen University in China for independently counting apoptotic index under microscope in a

single-blinding manner. We thank other members of our laboratories for helpful discussion and comments. This work was supported by the Major Projects Incubator Program of the National key Basic Research Program of China (2012CB526700), the National Natural Science Foundation of China (U1501224, 81370511), the International Cooperative Innovative Platform Guangdong Province Universities and College (gjhz1101).

Author contributions

Conceived and designed the experiments: BW and ZL. Performed the experiments: ZL, HT and JJ. Analyzed the data: BW, ZL, HT, YY, ST, LT, XL and HL. Contributed reagents/materials/analysis tools: BW. Wrote the manuscript: ZL and BW.

1. Andreyev HJ, Benton BE, Lalji A, Norton C, Mohammed K, Gage H *et al.* Algorithm-based management of patients with gastrointestinal symptoms in patients after pelvic radiation treatment (ORBIT): a randomised controlled trial. *Lancet* 2013; **382**: 2084–2092.
2. Hua G, Thin TH, Feldman R, Haimovitz-Friedman A, Clevers H, Fuks Z *et al.* Crypt base columnar stem cells in small intestines of mice are radioresistant. *Gastroenterology* 2012; **143**: 1266–1276.
3. Giannakis M, Stappenbeck TS, Mills JC, Leip DG, Lovett M, Clifton SW *et al.* Molecular properties of adult mouse gastric and intestinal epithelial progenitors in their niches. *J Biol Chem* 2006; **281**: 11292–11300.
4. Stappenbeck TS, Mills JC, Gordon JI. Molecular features of adult mouse small intestinal epithelial progenitors. *Proc Natl Acad Sci USA* 2003; **100**: 1004–1009.
5. Sato T, Vries RG, Snippert HJ, van de Wetering M, Barker N, Stange DE *et al.* Single Lgr5 stem cells build crypt–villus structures *in vitro* without a mesenchymal niche. *Nature* 2009; **459**: 262–265.
6. Potten CS. Radiation, the ideal cytotoxic agent for studying the cell biology of tissues such as the small intestine. *Radiat Res* 2004; **161**: 123–136.
7. Ch'ang HJ, Maj JG, Paris F, Xing HR, Zhang J, Truman JP *et al.* ATM regulates target switching to escalating doses of radiation in the intestines. *Nat Med* 2005; **11**: 484–490.
8. Paris F, Fuks Z, Kang A, Capodieci P, Juan G, Ehleiter D *et al.* Endothelial apoptosis as the primary lesion initiating intestinal radiation damage in mice. *Science* 2001; **293**: 293–297.
9. Rotolo J, Stancevic B, Zhang J, Hua G, Fuller J, Yin X *et al.* Anti-ceramide antibody prevents the radiation gastrointestinal syndrome in mice. *J Clin Invest* 2012; **122**: 1786–1790.
10. Neta R. Modulation of radiation damage by cytokines. *Stem Cells* 1997; **15**(Suppl 2): 87–94.
11. Riehl T, Cohn S, Tessner T, Schloemann S, Stenson WF. Lipopolysaccharide is radioprotective in the mouse intestine through a prostaglandin-mediated mechanism. *Gastroenterology* 2000; **118**: 1106–1116.
12. Linard C, Ropenga A, Vozenin-Brotons MC, Chapel A, Mathe D. Abdominal irradiation increases inflammatory cytokine expression and activates NF-kappaB in rat ileal muscularis layer. *Am J Physiol Gastrointest Liver Physiol* 2003; **285**: G556–G565.
13. Yeoh AS, Bowen JM, Gibson RJ, Keefe DM. Nuclear factor kappaB (NFkappaB) and cyclooxygenase-2 (Cox-2) expression in the irradiated colorectum is associated with subsequent histopathological changes. *Int J Radiat Oncol Biol Phys* 2005; **63**: 1295–1303.
14. Egan LJ, Eckmann L, Greten FR, Chae S, Li ZW, Myhre GM *et al.* IkappaB-kinasebeta-dependent NF-kappaB activation provides radioprotection to the intestinal epithelium. *Proc Natl Acad Sci USA* 2004; **101**: 2452–2457.
15. Wang Y, Meng A, Lang H, Brown SA, Konopa JL, Kindy MS *et al.* Activation of nuclear factor kappaB *in vivo* selectively protects the murine small intestine against ionizing radiation-induced damage. *Cancer Res* 2004; **64**: 6240–6246.
16. Linard C, Marquette C, Mathieu J, Pennequin A, Clarençon D, Mathé D. Acute induction of inflammatory cytokine expression after gamma-irradiation in the rat: effect of an NF-κB inhibitor. *Int J of Radiat Oncol Biol Phys* 2004; **58**: 427–434.
17. Zheng C, Yin Q, Wu H. Structural studies of NF-kappaB signaling. *Cell Research* 2011; **21**: 183–195.
18. Burdelya LG, Krivokrysenko VI, Tallant TC, Strom E, Gleiberman AS, Gupta D *et al.* An agonist of toll-like receptor 5 has radioprotective activity in mouse and primate models. *Science* 2008; **320**: 226–230.
19. Lefkowitz RJ, Whalen EJ. Beta-arrestins: traffic cops of cell signaling. *Curr Opin Cell Biol* 2004; **16**: 162–168.
20. Kim KS, Abraham D, Williams B, Violin JD, Mao L, Rockman HA. β-Arrestin-biased AT1R stimulation promotes cell survival during acute cardiac injury. *Am J Physiol Heart Circ Physiol* 2012; **303**: H1001–H1010.
21. Yang X, Zhou G, Ren T, Li H, Zhang Y, Yin D *et al.* β-Arrestin prevents cell apoptosis through pro-apoptotic ERK1/2 and p38 MAPKs and anti-apoptotic Akt pathways. *Apoptosis* 2012; **17**: 1019–1026.
22. Li H, Sun X, LeSage G, Zhang Y, Liang Z, Chen J *et al.* β-Arrestin 2 regulates Toll-like receptor 4-mediated apoptotic signalling through glycogen synthase kinase-3β. *Immunology* 2010; **130**: 556–563.
23. Wang P, Gao H, Ni Y, Wang B, Wu Y, Ji L *et al.* Beta-arrestin 2 functions as a G-protein-coupled receptor-activated regulator of oncoprotein Mdm2. *J Biol Chem* 2003; **278**: 6363–6370.
24. Hara MR, Kovacs JJ, Whalen EJ, Rajagopal S, Strachan RT, Grant W *et al.* A stress response pathway regulates DNA damage through β2-adrenoreceptors and β-arrestin-1. *Nature* 2011; **477**: 349–353.
25. Mittal N, Tan M, Eqbuta O, Desai N, Crawford C, Xie CW *et al.* Evidence that behavioral phenotypes of morphine in β-arr2-/-mice are due to the unmasking of JNK signaling. *Neuropsychopharmacology* 2012; **37**: 1953–1962.
26. Wang Y, Meng A, Lang H, Brown SA, Konopa JL, Kindy MS *et al.* Association of beta-arrestin and TRAF6 negatively regulates Toll-like receptor-interleukin 1 receptor signaling. *Nat Immunol* 2006; **7**: 139–147.
27. Zhou H, Ivanov VN, Lien YC, Davidson M, Hei TK. Mitochondrial function and nuclear factor-B-mediated signaling in radiation-induced bystander effects. *Cancer Res* 2008; **68**: 2233–2240.
28. Qiu W, Carson-Walter EB, Liu H, Epperly M, Greenberger JS, Zambetti GP *et al.* PUMA regulates intestinal progenitor cell radiosensitivity and gastrointestinal syndrome. *Cell Stem Cell* 2008; **2**: 576–583.
29. Kim SB, Pandita RK, Eskiocak U, Ly P, Kaisani A, Kumar R *et al.* Targeting of Nrf2 induces DNA damage signaling and protects colonic epithelial cells from ionizing radiation. *Proc Natl Acad Sci USA* 2012; **109**: E2949–E2955.
30. Suit HD, Withers HR. Endothelial cells and radiation gastrointestinal syndrome. *Science* 2001; **294**: 1411.
31. Russo SM, Tepper JE, Baldwin AS Jr, Liu R, Adams J, Elliott P *et al.* Enhancement of radiosensitivity by proteasome inhibition: implications for a role of NF-kappa B. *Int J Radiat Oncol Biol Phys* 2001; **50**: 183–193.
32. Jones RM, Sloane VM, Wu H, Luo L, Kumar A, Kumar MV *et al.* Flagellin administration protects gut mucosal tissue from irradiation-induced apoptosis via MKP-7 activity. *Gut* 2011; **60**: 648–657.
33. Leibowitz BJ, Qiu W, Liu H, Cheng T, Zhang L, Yu J. Uncoupling p53 functions in radiation-induced intestinal damage via PUMA and p21. *Mol Cancer Res* 2011; **9**: 616–625.
34. Lin C, Song L, Gong H, Liu A, Lin X, Wu J *et al.* Intestinal epithelial vitamin D receptor signaling inhibits experimental colitis. *J Clin Invest.* 2013; **123**: 3983–3996.
35. Kirsch DG, Santiago PM, di Tomaso E, Sullivan JM, Hou WS, Dayton T *et al.* P53 controls radiation-induced gastrointestinal syndrome in mice independent of apoptosis. *Science* 2010; **327**: 593–596.
36. Yu MC, Su LL, Zou L, Liu Y, Wu N, Kong L *et al.* An essential function for beta-arrestin 2 in the inhibitory signaling of natural killer cells. *Nat Immunol* 2008; **9**: 898–907.
37. Barker N, van Es JH, Kuipers J, Kujala P, van den Born M, Cozijnsen M *et al.* Identification of stem cells in small intestine and colon by marker gene Lgr5. *Nature* 2007; **449**: 1003–1007.
38. Qiu W, Wang X, Buchanan M, He K, Sharma R, Zhang L *et al.* ADAR1 is essential for intestinal homeostasis and stem cell maintenance. *Cell Death Dis* 2013; **4**: e599.
39. Wang P, Gao H, Ni Y, Wang B, Wu Y, Ji L *et al.* Beta-arrestin 2 functions as a G-protein-coupled receptor-activated regulator of oncoprotein Mdm2. *J Biol Chem* 2003; **278**: 6363–6370.
40. Wu B, Qiu W, Wang P, Yu H, Cheng T, Zambetti GP *et al.* P53 independent induction of PUMA mediates intestinal apoptosis in response to ischaemia–reperfusion. *Gut* 2007; **56**: 645–654.
41. Lin C, Song L, Gong H, Liu A, Lin X, Wu J *et al.* Nkx2-8 downregulation promotes angiogenesis and activates NF-κB in esophageal cancer. *Cancer Res* 2013; **73**: 3638–3648.
42. Potten CS. A comprehensive study of the radiobiological response of the murine (BDF1) small intestine. *Int J Radiat Biol* 1990; **58**: 925–973.
43. Roberts SA, Potten CS. Clonogen content of intestinal crypts: its deduction using a microcolony assay on whole mount preparations and its dependence on radiation dose. *Int J Radiat Biol* 1994; **65**: 477–481.
44. Withers HR, Elkind MM. Radiosensitivity and fractionation response of crypt cells of mouse jejunum. *Radiat Res* 1969; **38**: 598–613.

Supplementary Information accompanies this paper on Cell Death and Differentiation website (http://www.nature.com/cdd)